

Calculation of the local buckling in compression by the section damage method “case of the standardized profiles”

BARAKA Abdelhak^{1*}, BEKKAR Izzeddine¹, TAB Bounoua¹

¹LFGM Laboratory, Civil engineering department, University of TAHRI Mohamed, Bechar, Algeria

*Corresponding author: baraka.abdelhak@univ-bechar.dz

Abstract

Local buckling in metal sections is such a threat that Eurocode 3 imposes a passage through the classification of the section before any verification of the resistance of the structural elements. This characterization process is not necessary for flexural design (all sections are class 1). While in compression, their areas have different strength classes, several of which are class 4. This work focuses on studying merchant profiles subject to the risk of local buckling in compression. The neglected (ineffective) part of their sections is supposed to be damaged, which allowed us to associate this local instability with the damage parameter. There, it was necessary to appeal to the damage mechanic notions to formulate the evolution of the local instability of the thin wall of a metallic section. This simplifying approach is proposed to directly obtain the effective characteristics of the normalized areas via a damage parameter (D_c) without resorting to the classification of the sections and the effective calculation. The results obtained led us to propose two empirical and predictive models of the damage parameter associated with local buckling. The latter was validated by an analytical calculation and subjected to a statistical analysis of their accuracy.

Keywords : Local buckling, Effective section, Hot rolled profiles, Damage parameter, Class of section.

1. Introduction

Buckling is a phenomenon of instability of thin plates stressed in their plane [1-19]. It can occur by transverse compression of a plate [4], by bending in the plane of a plate or by shearing in the plane of the plate [4]. This instability is manifested by undulations parallel to the compression, as

if it were a transverse buckling of the plate, with the difference that the buckling develops more slowly [3-19].

Under local compression, local buckling is the first instability threatening the thin plate element of metal profiles. To avoid this, Eurocode 3 recommends first going through a classification of the sections, in

order to determine the exploitation area of the element. This process is based on the following criteria:

- Slenderness of the plate element (defined by width/thickness ratio);
- The distribution of compressive stresses, uniform or linear;
- Design resistance and plastic rotational capacity;

Hence the EC3 classification defines four classes of cross sections. The following Fig.1, shows the flexural strength and the rotational capacity that can be achieved by each class before the appearance of the local buckling phenomenon.

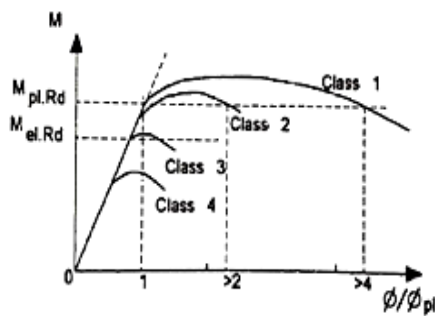


Fig.1. Section behaviour curves [4]

Due to their wide use, hot-rolled I-sections have been designed in such a way as to avoid a many number of instabilities (local buckling in bending, web buckling by shear). However, in normal compression some of their sections have weaknesses in the face of the risk of local buckling (Fig. 2.). Therefore, it is up to them to be classified according to paragraph 5.5 of part 1-1 of EC3 [20].

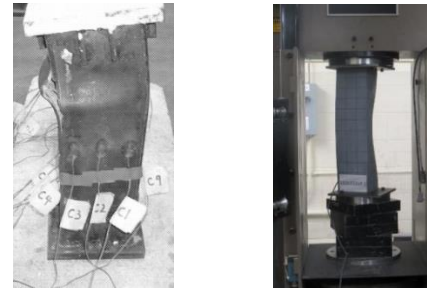


Fig. 2.Local buckling of the thin walls of section [5, 6].

Knowing that in simple compression the resistance provided by a section of the plastic row (Class 1 or 2) does not differ from the elastic one (of class 3) :

$$N_{pl,Rd} = \frac{A \cdot f_y}{\gamma_{M0}} \quad (1)$$

One can be satisfied with the values which delimit them from the effective calculation; which are:

For a compressed web;

$$\frac{d}{t_w} \leq 42 \quad (2)$$

For a compressed console of flange;

$$\frac{c}{t_f} \leq 14 \cdot \epsilon \quad (3)$$

The exception made by a class 4, obliges to pass to effective calculation

$$N_{eff,Rd} = \frac{A_{eff} \cdot f_y}{\gamma_{M1}} \quad (4)$$

In Euro code geometrical characterization (EN 1993-1-5, 5.2.2.) [21], one neglects a part of the section (Fig.3.), to be limited to a resistance lower than that which causes the buckling of a plate element. Thus, we will talk of effective resistance (Eq. 4).

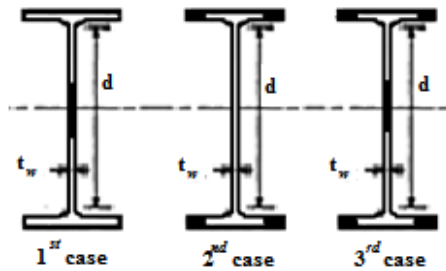


Fig.3. Effective calculations case for class 4 sections.

2. Calculation of cross sections

Profiles subject to local buckling in compressed areas, either by their significant height (upper part of the web in flexion, the entire web in compression) or excessive width (flange), must be subjected to the theoretical reduction of their section. The methodology to be followed for the determination of the geometric characteristics modified by the local buckling effect for a section of class 4, is explained in what follows; knowing that in simple compression $\psi = 1$ (flanges and/or the web are comprised).

- The reduced slenderness of the wall considered is calculated $\bar{\lambda}_p$ [21];

$$\bar{\lambda}_p = \left[\frac{f_y}{\sigma_{cr}} \right]^{0,5} = \frac{\left(\frac{\bar{b}}{t} \right)}{28,4 \cdot \varepsilon \cdot \sqrt{k_\sigma}} \quad (5)$$

t : plate thickness.

The width of the plate element considered;

$$\bar{b} = d \quad \text{for webs}$$

$$\bar{b} = C = b/2 \quad \text{for flanges of rolled profile.}$$

The ratio;

$$\varepsilon = \sqrt{\frac{235}{f_y \text{ (N/mm}^2)}} \quad (6)$$

The buckling coefficient

$$k_\sigma = f(\psi) \quad [21].$$

For the Web in simple compression;

$$k_\sigma = 0,43$$

For the Flange in simple compression;

$$k_\sigma = 4,0$$

Determination ρ ;

$$\text{if : } \bar{\lambda}_p \leq 0,673 \rightarrow \rho = 1. \quad (7)$$

$$\text{if not } \bar{\lambda}_p > 0,673 \rightarrow \rho = \frac{(\bar{\lambda}_p - 0,22)}{\bar{\lambda}_p^2} \quad (8)$$

The effective width of the plate element:

$$b_{eff} = \rho \cdot \bar{b} \quad (9)$$

The effective width (b_{eff}) is the hatched part in the Fig.4, and the width of the neglected parts (b_{neg}) becomes;

$$b_{neg} = (1-\rho) \cdot \bar{b} \quad (10)$$

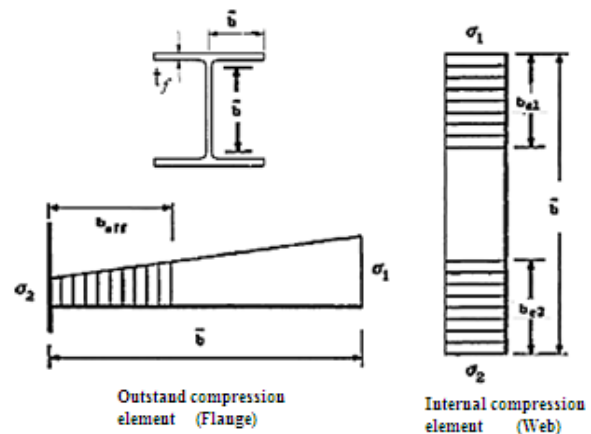


Fig.4. Stress distribution and effective width for the plate elements [21]

After classification under compression of classic hot-rolled sections, we identified those which have a class 4 section

(Table. 1.). Then, we determined for each of these last its effective cross section.

Table. 1. Rolled sections I and H of class 4 in compression.

Steel grade	S235	S275	S355	S460
IPE	550 to 600	450 to 600	300 to 600	220 to 600
IPE A	360 to 600	270 to 600	200 to 600	160 to 600
IPEO	-	-	450 to 600	300 to 600
HEA	800to 1000	650 to 1000	550 to 1000	280 & 500 to 1000
HEA-A	650 to 1000	280 to 300	200 to 360	120 to 1000
			450 to 1000	
HEB	1000	900 to 1000	700 to 1000	600 to 1000
HEM	-	1000	900 to 1000	800 to 1000

3. Concept of damage section

The use of damage mechanics has so far been devoted to the field of fragile materials. Damage approaches mainly involve two stages:

- Choice of the variables of the damage to characterize the state of damage of the material.
- Establishment of the law of evolution for the damage variables chosen [22].

In its foundation, the mechanics of damage constitutes a modelling tool which is

applicable for many failure mechanisms and for a large number of families of material behaviours. The damage can be introduced as a measure of all the physical degradations (cracks...) or mechanical (reduction of the tangent modulus....). Thus, one can define a parameter of damage (D) such that its value is null in the absence of damage, and is equal to one if it is total, ie the effective resistance of section become zero ($A_{eff} = 0$).

We thus set [22];

$$D = 1 - \frac{A_{eff}}{A} \quad (11)$$

This notion can be generalized in the case of a constraint by the following formula; called effective constraint [22,23].

$$\{\sigma\} = \frac{\{\sigma\}}{1-D} \quad (12)$$

And with E the Hooke tensor characterizing the elasticity of the material, one deduces from it the expression of the tensor of effective Hooke of the damaged material (Eq. 13) [22]:

$$\tilde{E} = E(1 - D) \quad (13)$$

2.1.Adaptation of the damage mechanics to our problem

From the notions offered by the expression (Eq.12), we can also use the damage parameter in the field of the stability of the metallic elements so as to consider the local buckling as being a mechanical damage undergone in the plastic behaviour of conventional sections (Eq. 14).

$$N_{eff,Rd} = N_{pl,Rd} \cdot (1 - D) \quad (14)$$

Thus, the goal of this work consists in directly deducing the effective section

starting from the parameter of damage in compression (Eq. 15).

$$A_{eff} = A.(1-D) \quad (15)$$

By calculating the effective sections for the classic profiles of class 4 in compression (Table. 1.), one will follow the evolution of the damage parameter (D) according to the ratio (d/t_w). It should be noted that for these profiles the reduction of the section occurs only at web.

2.2. Damage parameter associated at buckling

After determining the ineffective widths for slanders elements (Eq.16), the neglected sections can be calculated as follows;

$$\text{Web: } A_{w,neg} = d_{neg} \cdot t_w \quad (16)$$

$$\text{Flange: } A_{f,neg} = C_{neg} \cdot t_f \quad (17)$$

For the total effective section (Fig. 3.3rd case) :

$$A_{eff} = A - A_{w,neg} - 4 \cdot A_{f,neg} \quad (18)$$

Table. 2. The variation of the damage parameter in compression of IPE profile.

Profile IPE				
Grade	Profile	d/t _w	A _{eff,EC3} (cm ²)	D _{c,EC3} %
S235	550	42,13	131.32	2,00
	600	42,83	152.25	2,40
S275	450	40,30	96.29	2,54
	500	41,76	112.07	3,39
	550	42,13	129.05	3,69
	600	42,83	149.54	4,14
	S355	300	35,01	52.68

	330	36,13	60.96	2,63
	360	37,33	70.33	3,26
	400	38,49	81.18	3,92
	450	40,30	93.72	5,14
	500	41,76	108.92	6,10
	550	42,13	125.29	6,50
	600	42,83	145.07	7,01
	S460	220	30,10	32.86
240		30,71	38.36	1,887
270		33,27	44.34	3,391
300		35,01	51.39	4,471
330		36,13	59.47	5,005
360		37,33	68.58	5,671
400		38,49	79.09	6,400
450		40,30	91.11	7,779
500		41,76	105.75	8,833
550		42,13	121.51	9,320
600	42,83	140.59	9,878	

From there, one determines the damage parameter in compression by assimilating it to the failed part of the section according to Eurocode 3. And starting from the equation (Eq. 11), (Eq. 15), we obtain the following relation (Eq. 19) between the effective sections and the damage parameter.

The damage parameter becomes:

$$\frac{A_{eff}}{A} = 1 - D \Rightarrow D = 1 - \frac{A_{eff}}{A} \quad (19)$$

Although the calculation was made for all the classic rolled sections (I, H), we are content to present in this paper the variations of the damage parameter

$(D_{c,EC3})$ associated with the effective section obtained by EC3 ($A_{eff, EC3}$) for IPE profiles with conventional steel grades (Table. 2.). The change in the damage parameter, for IPE rolled sections as a function of the (d/t_w) ratio, has a quasi-linear form for each grade (Fig.5.).

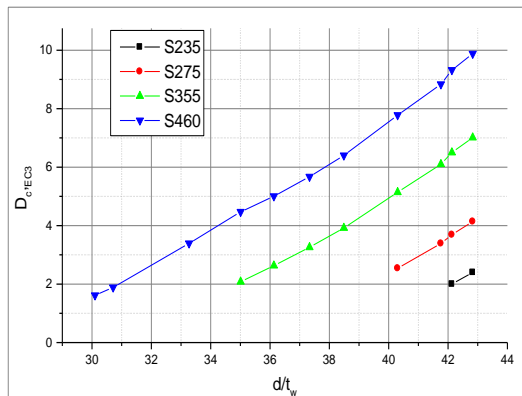


Fig. 5. Damage parameter in compression of hot rolled profile IPE.

The same, the change in the damage parameter for IPE_A rolled sections takes similar form (Fig.6.).

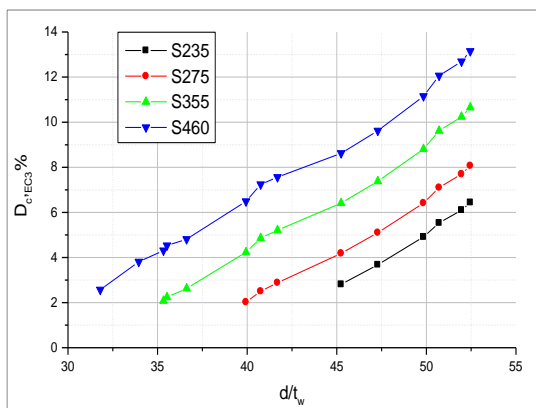


Fig. 6. Damage parameter in compression of profile IPE_A.

For HE profiles, since the neglected part is located at the web (Fig.3.1st case), the functions found have practically the same appearance as that of the IPE. The

exception is made by the HEA-A profiles which, in addition to that of the web, undergo an effective calculation even for the flanges (Fig.3.3rd case).

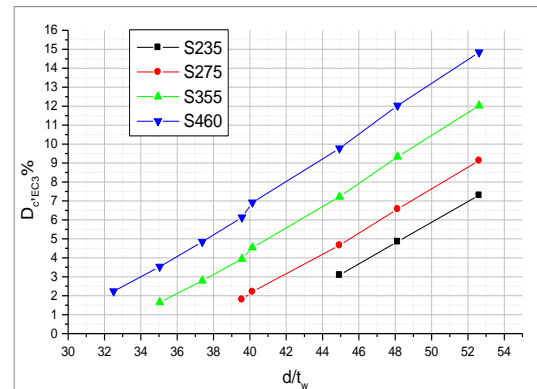


Fig. 7. Damage parameter in compression of HEA profile.

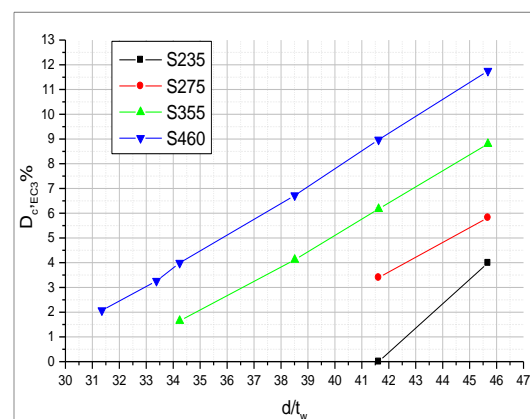


Fig. 8. Damage parameter in compression of HEB profile.

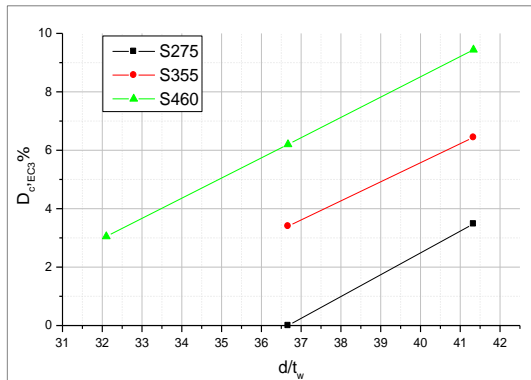


Fig. 9. Damage parameter in compression of HEM profile.

This variation of the damage parameter keeps the same appearance for all Classic profiles (IPE, IPEA, IPEO, HEA, HEA-A, HEB, HEM). Then, we propose a descriptive law by following linear form :

$$D_{c,DSM} = A \cdot \frac{d}{t_w} + B \quad (20)$$

To take into account the steel grade, we integrate the grade coefficient into the previous equation (Eq. 6.). The fitting function that is suitable for varying the compression damage parameter, for all rolled sections, takes the form:

$$D_{c,DSM} \% = \left(\frac{1}{\sqrt[6]{\varepsilon}} \right) \left[\frac{A}{\varepsilon} \cdot \left(\frac{d}{t_w} \right) - \frac{B}{\sqrt{\varepsilon}} \right] \quad (21)$$

We also noted that the variation of the slope, of the damage parameter, is almost constant and takes the value **A = 0,571**. The fitting function becomes

$$D_{c,DSM} \% = \left(\frac{1}{\sqrt[6]{\varepsilon}} \right) \left[\frac{0,571}{\varepsilon} \cdot \left(\frac{d}{t_w} \right) - \frac{B}{\sqrt{\varepsilon}} \right] \quad (22)$$

For the value of “B”, two methods have been proposed for its determination:

The first formula gives the variation of “B” by an equation (Eq. 23). In the second, the value of “B” for each profile is given in Table. 3.

Model 1: We evaluate D_c by calculating the value of “B” with the following formula;

$$B = 21,2 \times 1,2^{\left(1 - \frac{t_w}{15,5}\right)} \quad (23)$$

Model 2 : We calculate D_c , taking the value of “B” directly from the Table 3.2.

Table. 3. The values of “B” of each profile according to DSM.

Profile	B
IPE_A	23,5
IPE	22,055
IPE_O	22
HEA_A	21,42
HEA	22,7
HEB	22,1
HEM	22,6

4. Validation of model

We implemented the proposed formulations (Eq. 22) and (Eq. 23) in Excel, the ratio (d/t_w) of each profile was introduced to obtain the damage parameter with which the effective section is directly calculated. The graphical representation of the results is made by points, because indeed the computation values (d/t_w) are discrete.

All results of the IPE profiles are presented. For IPE-A, IPE-O and for HE profiles, we present here one case of each type, which will give an idea of the accuracy of the fitting function.

Due to the fact that the effective calculation affects the flanges for the HEA-A profiles (class 4), the formulation requires a complement to cover this case,

so we have contented with representing the results of the other profiles.

For the IP and HE profiles the results of the correlation are shown in Fig.10. to Fig.18. The analysis of the precision of the models was made by the ratio R^2 (the ratio of the sum of the squares of the predicted responses to the sum of the squares of the experimental responses) which is close to one, if the predicted responses are representative.

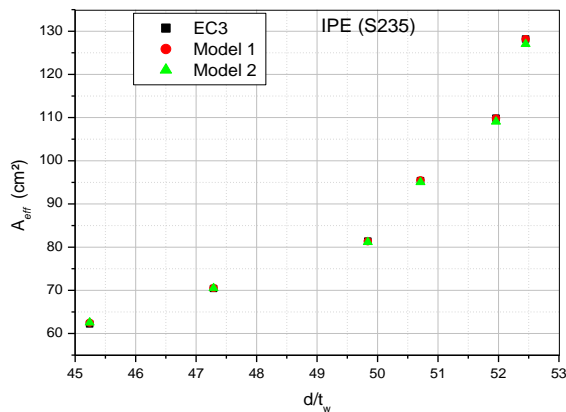


Fig. 10. Comparison of A_{eff} between models and EC3 for IPE (S235).

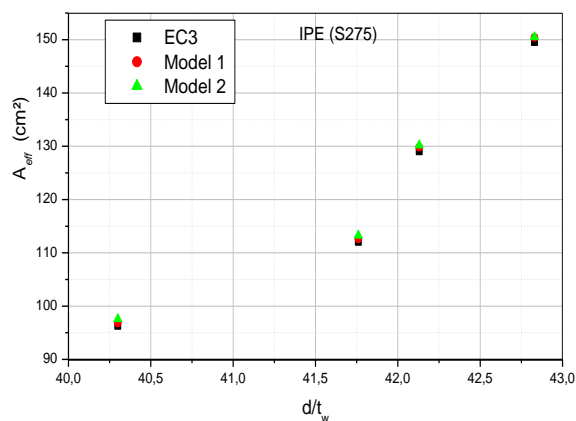


Fig. 11. Comparison A_{eff} of models and EC3 for IPE (S275).

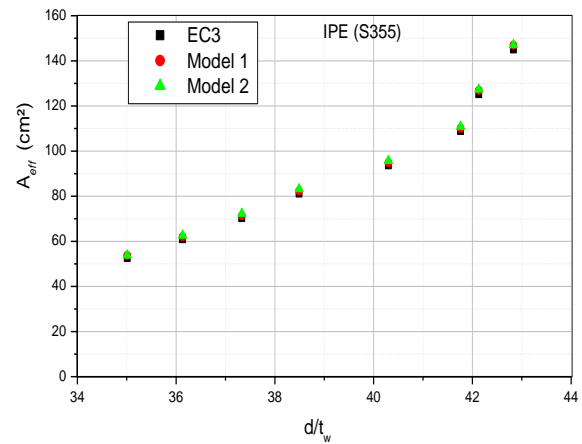


Fig. 12. Comparison A_{eff} of models and EC3 for IPE (S355).

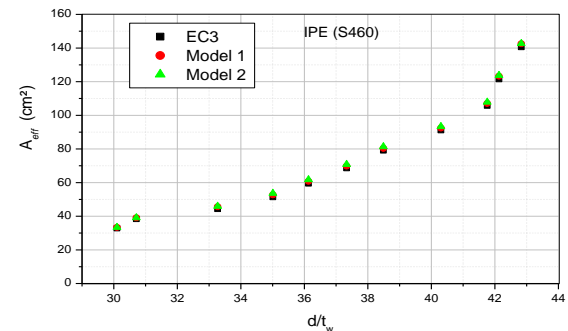


Fig. 13. Comparison of A_{eff} between models and EC3 for IPE (S460).

For the IPE-A and IPE-O profiles, the formulation shows a good correlation.

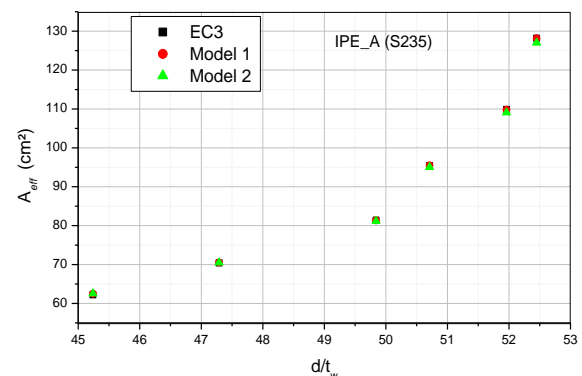


Fig. 14. Comparison of A_{eff} of models and EC3 for IPE_A (S235).

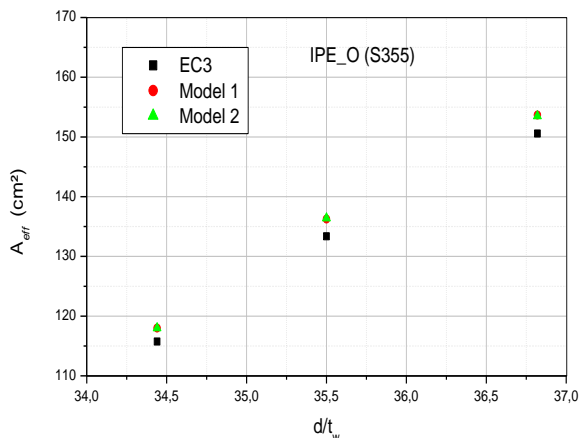


Fig. 15. Comparison of A_{eff} between models and EC3 for IPE_O (S355).

Fig. 17. Comparison of A_{eff} between models and EC3 for HEB (S275).

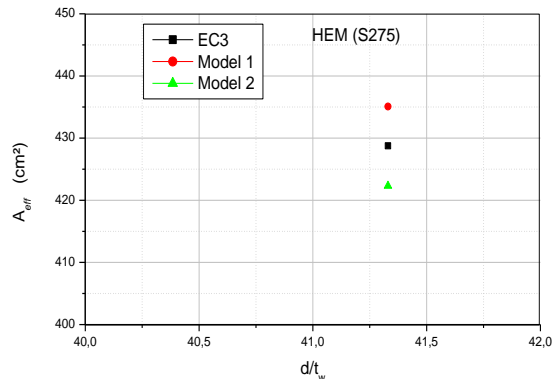


Fig. 18. Comparison A_{eff} of the models and EC3 for HEM1000 (S275).

HE profiles have a more compact section and the results remain satisfactory.

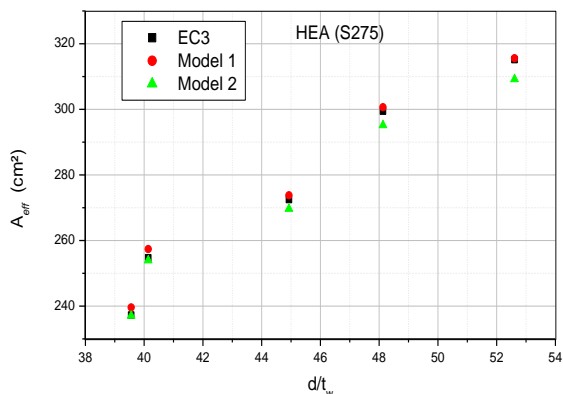
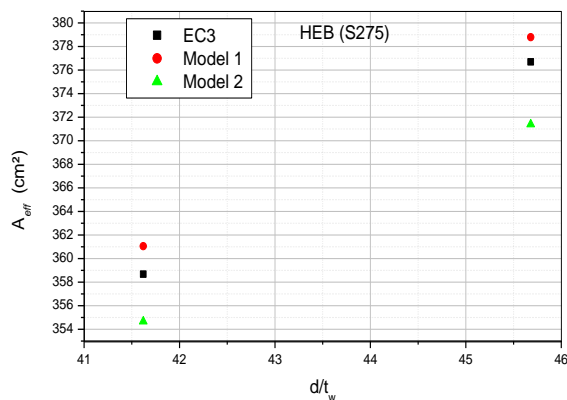


Fig. 16. Comparison A_{eff} of models and EC3 for HEA (S275).



According to this formula, we see that the R^2 ratio is close to 1 (Table. 4.), which means that the model perfectly predicts the data responses (EC3).

Table. 4. Absolute errors R^2 of the different "I" hot rolled profiles.

Profile	Grade	S235	S275	S355	S460
IPE	Model 1	1,000	1,006	0,930	1,017
	Model 2	1,001	1,009	1,020	1,024
IPE_A	Model 1	1,001	1,004	1,005	0,999
	Model 2	0,996	1,001	1,001	0,996
IPE_O	Model 1	-	-	1,021	0,984
	Model 2	-	-	1,019	0,984
HEA	Model 1	1,001	1,004	1,005	0,999
	Model 2	0,996	1,001	1,001	0,996
HEB	Model 1	1,000	1,006	0,738	1,020
	Model 2	0,982	0,987	0,997	1,030
HEM	Model 1	-	1,015	1,027	1,033
	Model 2	-	0,985	0,994	1,001

5. Example of effective section calculation with DSM method

In this section an example involving I-section is given, to accommodate how the simplified method of damaged section could be employed to compute the properties (A_{eff}) of a class 4 section in compression.

5.1. Example

For the profile HEB800 (S275), $D_{c,EC3} = 0$ so there is no effective calculation. Then, **Eurocode 3** : Resistant force for HEB 800;

$$N_{pl,Rd} = \frac{A \cdot f_y}{\gamma_{M0}} = \frac{33420 \cdot 275}{1}$$

$$= 9190500 \text{ N} = 9190,5 \text{ KN}$$

For a profile HEB 800 (S460 $\Rightarrow \epsilon = 0,77$),

$$d = 12 \text{ mm and } t_w = 15 \text{ mm}$$

From the effective calculation of the section following EC3 (See paragraph 2.), we found:

$$A_{eff} = 311,75 \text{ cm}^2$$

Then the effective resistance force is equal:

$$N_{eff,Rd} = \frac{A_{eff} \cdot f_y}{\gamma_{M1}} = \frac{31175 \times 460}{1,1}$$

$$= 13036818,2 \text{ N} = 13036,81 \text{ KN.}$$

Damage Section Method : With this Method (DSM), by taking the value of $B = 22,1$; from Table. 3, the application of equation (Eq. 22) gives;

$$D_c\% = \left(\frac{1}{\sqrt{0,77}} \right) \left[\frac{0,571}{0,77} \cdot \left(\frac{12}{15} \right) - \frac{22,1}{\sqrt{\epsilon}} \right]$$

$$= 6,64\% > 0 ;$$

\rightarrow the section is necessarily of class 4.

So, we must calculate the cross section (Eq. 15), as follows:

$$A_{eff,DSM} = (1 - D_c) \times A$$

From where :

$$A_{eff,DSM} = 33420 \times (1 - 0,0664)$$

$$= 31200,912 \text{ mm}^2$$

The effective resistant force is equal to :

$$N_{eff,DSM,Rd} = \frac{A_{eff,DSM} \cdot f_y}{\gamma_{M1}} = \frac{31200 \times 460}{1,1}$$

$$= 13047272,7 \text{ N} = 13047,27 \text{ KN.}$$

In this case, the error on the resistant force is of the order of 0,08 %.

With a similar error rate for all rolled I and H sections, the model can be said to be reliable.

6. Conclusions

With the application of the concept of effective design in EC 3, most of the section tables of rolled sections lack data relating to the design of effective parts. In compression, the stages of the classification of these sections and their effective calculation, of which the EC3 regulation devotes a whole part, become compulsory. Our contribution comes within the context of reducing these steps, by representing the local buckling phenomenon by a single variable, called "Damage parameter D_c ".

For this purpose, we have separately studied rolled sections subject to local buckling. Then, two models were proposed on the basis of the damage mechanics. The approach consists in calculating the effective section via the parameter of damage D_c , without recourse neither to the

classification of the sections not to the effective calculation. It considers that the section is of class 4, if it is likely to be damaged, that is to say:

If $D_c > 0$ the section is class 4

(Effective calculation).

If not $D_c \leq 0$ the section is class

1, 2 or 3 (Under compression).

Thus, the formulation developed (Eq. 22), (Eq. 23) simplified the calculation of the effective part. A static analysis of the results showed that they are acceptable, and that the first model is better than the second, this for all rolled sections.

Finally, this concept can easily be implemented in the finite element method, by integrating it into the stiffness matrix of the material. We hope that this notion of the damage mechanic will be improved to cover all cases of effective design in steel sections (bending, and compression for welded sections).

References

- [1] Von Karman, T., E. E. Sechler, and L. H. Donnell, The Strength of Thin Plates in Compression. Transactions, ASME, vol. 54, APM 5405, 1932.
- [2] Winter, G., Strength of Thin Steel Compression Flanges. Transactions of ASCE, Paper No. 2305, Trans., 112, 1, 1947.
- [3] MANFRED A , HIRT Rolf Bez ; construction métallique_ notions fondamentales et méthodes de dimensionnement. Traité de Génie Civil de l'Ecole polytechnique Fédérale, Lausanne, avril 1994.

- [4] JEAN MORAEL ; Calcul des structures métalliques selon l'Eurocode 3. Editions Eyrolles 61.bd Saint-Germain 75240 Paris, Sixième tirage 2005.
- [5] M. Mursi, Brayan Uy; Behavior and design of fabricated high strength steel columns subjected to biaxial bending – Part I : experiments; Advanced Steel Construction – Vol. 2 No. 4, 286–313; 2006.
- [6] F. Pourshargh, F. P. Legeron, and S. Langlois, Modeling the local buckling failure of angle sections with beam elements, Advanced Steel Construction – Vol. 15 No. 4, 364–376, 2019.
- [7] Chi-King Lee , Sing-Ping Chiew; A review of class 4 slender section properties calculation for thin-walled steel sections according to EC3; Advanced Steel Construction – Vol. 15 No. 3, 259–266; 2019
- [8] Gardner, L., Fieber, A., & Macorini, L. (2019, February). Formulae for calculating elastic local buckling stresses of full structural cross-sections. In Structures (Vol. 17, pp. 2-20). Elsevier.
- [9] Wagner, H. N. R., Köke, H., Dähne, S., Niemann, S., Hühne, C., & Khakimova, R. (2019). Decision tree-based machine learning to optimize the laminate stacking of composite cylinders for maximum buckling load and minimum imperfection sensitivity. Composite Structures, 220, 45-63.
- [10] Wagner, H. N. R., Petersen, E., Khakimova, R., & Hühne, C. (2019). Buckling analysis of an

- imperfection-insensitive hybrid composite cylinder under axial compression–numerical simulation, destructive and non-destructive experimental testing. *Composite Structures*, 225, 111152.
- [11] Evkin, A. (2021). Analytical model of local buckling of axially compressed cylindrical shells. *Thin-Walled Structures*, 168, 108261.
- [12] Wagner, H. N. R., Hühne, C., & Niemann, S. (2020). Buckling of launch-vehicle cylinders under axial compression: a comparison of experimental and numerical knockdown factors. *Thin-Walled Structures*, 155, 106931.
- [13] Evkin, A., & Lykhachova, O. (2021). Energy barrier method for estimation of design buckling load of axially compressed elasto-plastic cylindrical shells. *Thin-Walled Structures*, 161, 107454.
- [14] Fan, H., Gu, W., Li, L., Liu, P., & Hu, D. (2021). Buckling design of axially compressed cylindrical shells based on energy barrier approach. *International Journal of Structural Stability and Dynamics*, 21(12), 2150165.
- [15] Lykhachova, O., & Evkin, A. (2020). Effect of plasticity in the concept of local buckling of axially compressed cylindrical shells. *Thin-Walled Structures*, 155, 106965.
- [16] Krasovsky, V., & Evkin, A. (2021). Experimental investigation of buckling of dented cylindrical shells under axial compression. *Thin-Walled Structures*, 164, 107869.
- [17] Wagner, H. N. R., Hühne, C., & Khakimova, R. (2019). On the development of shell buckling knockdown factors for imperfection sensitive conical shells under pure bending. *Thin-Walled structures*, 145, 106373.
- [18] Wagner, H. N. R., Sosa, E. M., Ludwig, T., Croll, J. G. A., & Hühne, C. (2019). Robust design of imperfection sensitive thin-walled shells under axial compression, bending or external pressure. *International Journal of mechanical sciences*, 156, 205-220.
- [19] Groh, R. M. J., Hunt, G. W., & Pirrera, A. (2021). Snaking and laddering in axially compressed cylinders. *International Journal of Mechanical Sciences*, 196, 106297.
- [20] EN 1993-1-1 (2005); Eurocode 3 : Design of steel structures - Part 1-1: General rules and rules for buildings [Directive 98/34/EC, Directive 2004/18/EC]
- [21] EN 1993-1-5 (2006); Eurocode 3 : Design of steel structures - Part 1-5: General rules - Plated structural elements [Directive 98/34/EC, Directive 2004/18/EC].
- [22] DOMINIQUE FRANCOIS; Endommagements et rupture des matériaux. Ecole centrale de Paris, édition EDP Sciences, France, 2004.
- [23] Wu, J. Y., & Nguyen, V. P. (2018). A length scale insensitive phase-field damage model for brittle fracture. *Journal of the Mechanics and Physics of Solids*, 119, 20-42.
- [24] Van Do, V. N. (2016). The behavior of ductile damage model on steel structure failure. *Procedia engineering*, 142, 26-33.